GEOPHYSICS, VOL. 56, NO. 12 (DECEMBER 1991); P. 2070–2079, 8 FIGS.

Diffraction-based velocity estimates from optimum offset seismic data

Guy M. Cross* and Michael D. Knoll‡

ABSTRACT

A graphical method is characterized for estimating seismic velocity directly from diffraction patterns observed on common offset records. The nature of the resulting estimate is examined by illustrating the connection between the graphical approach and a related method used by practitioners of ground penetrating radar. While the latter provides only a crude stacking velocity, the graphical technique yields the generalized rms velocity for stratified media. Associated interval velocities can be derived from two or more diffraction events having their sources within the plane of survey. Where there is a lack of geological evidence to suggest that scatterers reside in-plane, we propose a simple strategy for locating a scatterer from its expression on two or more independent records. Error in the resulting location is directly related to subsurface velocity heterogeneity. Finally, since the diffraction-based velocity estimates assume that source and receiver are coincident, the error stemming from nonzero offset is characterized.

INTRODUCTION

The Terrain Geophysics Section of the Geological Survey of Canada pioneered and, since the early 1980s, has popularized the optimum offset technique for high resolution shallow seismic profiling (Hunter et al., 1984; Hunter and Pullan, 1989). The method relies on preliminary expanding offset noise tests to identify a range of source-receiver offsets over which the reflection from a given target interface is received with minimum interference from source-generated noise. An optimum offset, selected from within this range, is then used to acquire single fold soundings along profile.

Compared with suitably scaled CDP techniques (Knapp and Steeples, 1986; Steeples and Miller, 1988), optimum offset profiling is conceptually less complicated and has the advantage of requiring little, if any, post acquisition data processing to yield an interpretable result. In part, however, this advantage is sacrificed by the need to collect and analyze supplemental multifold data to determine a velocity function for depth conversion. To reduce the need for these additional data, we propose to make greater use of moveout information supplied by diffraction events to derive supplemental velocity estimates directly from common offset data. In addition, since these estimates require only a pencil and ruler, they represent a convenient source of velocity information in the field.

Diffraction-based velocity analysis is familiar to practitioners of ground penetrating radar (GPR) where data are acquired almost entirely in common offset mode. Here we characterize the relationship between a simple method used there and another more robust technique that leads naturally to a meaningful interval velocity function. Finally, while source and receiver components of GPR systems are often effectively coincident and seldom separated by more than a meter, this is not the case for optimum offset seismic acquisition. Consequently, we examine the effect of nonzero offset on transit time within a constant velocity medium and evaluate the corresponding influence on apparent velocity.

Previous studies (Dinstel, 1971; Larner et al., 1983; Tsai, 1984) have examined the appearance of scattered energy in a variety of acquisition and display formats, but have focused principally on CMP gathers and the suppression of these events by stacking and velocity filtering. We are concerned, instead, with diffractions in the common offset domain and the velocity implied by transit time moveout as a fixed spread traverses the scatterer.

POINT DIFFRACTIONS ON COMMON OFFSET RECORDS

Consider a point diffractor within a homogeneous, isotropic half-space as depicted in Figure 1. A rectangular coordi-

Manuscript received by the Editor October 3, 1990; revised manuscript received May 28, 1991.
*Department of Geophysics and Astronomy, University of British Columbia, Vancouver, V6T 1Z4, Canada.
‡Department of Geological Sciences, University of British Columbia, Vancouver, V6T 1Z4, Canada.

nate system is chosen so that scattered energy detected by an optimum offset survey along the x-axis has minimum arrival time when the spread midpoint is at the origin. With the spread so positioned, a line segment joining the scatterer and the midpoint is normal to profile and, consequently, minimum length. Note that this implies a scatterer residing in the yz-plane.

For source at $(X_S, 0, 0)$, receiver at $(X_R, 0, 0)$, and point diffractor at $(0, Y_D, Z_D)$, the appropriate transit time expression is

$$t = \frac{1}{V}\,[(X_S^2 + r^2)^{1/2} + (X_R^2 + r^2)^{1/2}], \tag{1}$$

where V is a constant velocity and $r = (Y_D^2 + Z_D^2)^{1/2}$ is the distance from the origin to the scatterer. Expressing source and receiver positions in terms of spread midpoint X_M and optimum offset $\Delta x = X_R - X_S$ as

$$\begin{aligned} X_S &= X_M - \Delta x/2 \\ X_R &= X_M + \Delta x/2 \end{aligned}, \tag{2}$$

we obtain the equivalent relation

$$t = \frac{1}{V}\,\{[X_M - \Delta x/2)^2 + r^2]^{1/2} + [(X_M + \Delta x/2)^2 + r^2]^{1/2}\}. \tag{3}$$

For the time being, we shall consider the case of coincident source-receiver. Setting $\Delta x = 0$ in equation (3) and squaring both sides yields for zero offset transit time

$$t^2 = t_0^2 + \frac{4X^2}{V^2}, \tag{4}$$

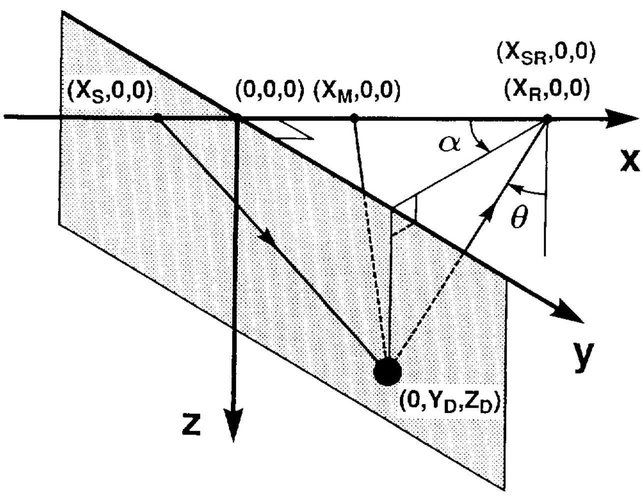

FIG. 1. Point scatterer model and reference coordinate system. X_S, X_M, and X_R denote source, midpoint, and receiver positions along the x-axis. Y_D and Z_D are, respectively, the y and z coordinates of a point diffractor residing in the yz-plane. X_{SR} denotes the position of a coincident source-receiver pair. θ and α are, respectively, takeoff and azimuthal angles for the ray joining $(X_{SR}, 0, 0)$ and $(0, Y_D, Z_D)$.

where $t_0 = 2r/V$ is the minimum arrival time for scattered energy detected by a coincident source-receiver. Although we have dropped the subscript on X_M to simplify notation, we remind the reader that this variable specifies midpoint position along profile and should not be confused with optimum offset, Δx. Having said this, however, note the obvious similarity between equation (4) and the CMP transit time relation for reflection from a dipping planar interface (Levin, 1971). In the latter case, transit time is measured as a function of offset about a constant midpoint rather than as a function of midpoint location for a common offset. Both events are hyperbolic.

VELOCITY ESTIMATES FROM DIFFRACTIONS

The diffraction pattern resulting for an arbitrary point scatterer is illustrated in Figure 2a. As for the case of reflections, a reasonable estimate of the constant velocity V can be obtained by exploiting the linearity of equation (4) in X^2 versus t^2 space. As depicted in Figure 2b, the diffraction hyperbola maps to a line having intercept t_0^2 and slope $4/V^2$. Rather than determine the arrival time of scattered energy at numerous midpoint locations and perform the required linear regression, practitioners of ground-penetrating radar have commonly pursued a more direct approach (Ulriksen, 1982; Daniels, 1989). Having identified the apex of a diffraction event $(0, t_0)$ together with any additional point (X, t) (Figure 2a), velocity is derived directly from equation (4) as

$$V^2 = \frac{4X^2}{(t^2 - t_0^2)}. \tag{5}$$

In effect, this amounts to specifying the intercept $(0, t_0^2)$ and a second point (X^2, t^2) on the line described by equation (4) and is, ideally, equivalent to the corresponding two-point slope estimate (Figure 2b). It follows that, in practice, velocity estimates obtained from equation (5) are particularly sensitive to measurement error associated with arrival times.

Implicit differentiation of equation (4) with respect to the midpoint variable X gives

$$V^2 = \frac{4X}{t}\frac{dX}{dt} = \frac{2X}{tp_x \cos\alpha}, \tag{6}$$

where $dt/dX = 2p_x \cos\alpha$ is the slope of a local tangent to the diffraction event at (X, t). The reader should recognize that p_x is the equivalent Snell parameter with $\alpha = \tan^{-1}(Y_D/X)$ denoting the azimuthal angle as depicted in Figure 1. As González-Serrano and Claerbout (1984) have demonstrated for the case of reflection events on CMP gathers, equation (6) suggests an alternative approach for estimating velocity directly from the constant offset record. In this approach, the interpreter must supply a local slope estimate but need not specify the minimum arrival time t_0 required by equation (5). Although the errors in these measurements are comparable, equation (6) is less prone to propagating transit time uncertainties. Also, by incorporating the local slope of the scattering event, equation (6), if only by eye, involves a sort of curve fitting to the entire event. Consequently, in addition to yielding velocity directly from the constant offset profile, we expect equation (6) to provide a relatively robust estimate.

Now, having set out the basic concepts assuming a uniform medium, let us examine the more interesting situation where velocity is vertically variable. It is in this context that we shall discover the connection between the two direct velocity estimates described above. Consider a point scatterer within a stack of horizontal isovelocity layers having thickness z_k and velocity v_k as depicted in Figure 3. Let us assume, for the moment, that scattered energy has taken the path of least distance from source to scatterer and back to the coincident receiver. Under this straight ray assumption, transit time is predicted exactly by equation (4) upon replacing the uniform velocity V by the appropriate average velocity

$$V_a = \frac{1}{T_0} \sum_{k=1}^{n} v_k \tau_k = \frac{2}{T_0} \sum_{k=1}^{n} z_k, \tag{7}$$

where $\tau_k = 2z_k/v_k$ is the two-way vertical transit time within the kth layer and

$$T_0 = \sum_{k=1}^{n} \tau_k = 2 \sum_{k=1}^{n} \frac{z_k}{v_k}. \tag{8}$$

Here, T_0 is the two-way transit time for an in-plane scatterer located vertically beneath the coincident source-receiver and should be distinguished from t_0, the minimum two-way transit time for an arbitrary scatterer. The two are equivalent only for a diffractor within the plane of survey ($\cos \alpha = 1$) as depicted in Figure 3. Now, if v_k and z_k are chosen so that $V_a = V$, the corresponding diffraction event and its mapping in X^2 versus t^2 are the same as for the case of uniform velocity in Figure 2. This is not surprising since equation (4) was derived under the same straight ray assumption. In short, all that we have said regarding the case of uniform velocity holds for stratified velocity, assuming that scattered energy takes the path of least distance. Most importantly, the velocity predicted by equations (5) and (6) remains constant for all values of X.

In practice, scattered energy reaching the receiver has actually taken the path of least time in accordance with Fermat's principle. Compared with the straight ray case, the path of least time reduces transit through lower velocity layers while increasing the distance traveled at higher velocities as suggested in Figure 3. Consequently, as the designation indicates, transit time via the least time path is always less than or equal that by the corresponding straight raypath. In particular, least time and least distance paths are equivalent only for an in-plane scatterer located vertically beneath the coincident source-receiver. Otherwise, as X increases, the actual two-way transit time is progressively less than that predicted, assuming straight ray geometry. This effect is illustrated in Figure 2a for an in-plane scatterer. The actual two-way transit time is denoted by t' for comparison with the corresponding least distance arrival time t for the same arbitrary midpoint location.

As for the case of reflection from a plane horizontal interface (Dix, 1955), the true diffraction event is nonlinear in X^2 versus t^2 (Figure 2b), indicating that equation (4) is, strictly speaking, inappropriate for stratified media. Despite this limitation, it follows from Dix's small spread analysis that for X small compared to depth, $Z_D = \Sigma_{k=1}^{n} z_k$, equation (4) yields a sufficiently accurate prediction of transit time when the uniform velocity V is replaced by the root-mean-square (rms) velocity

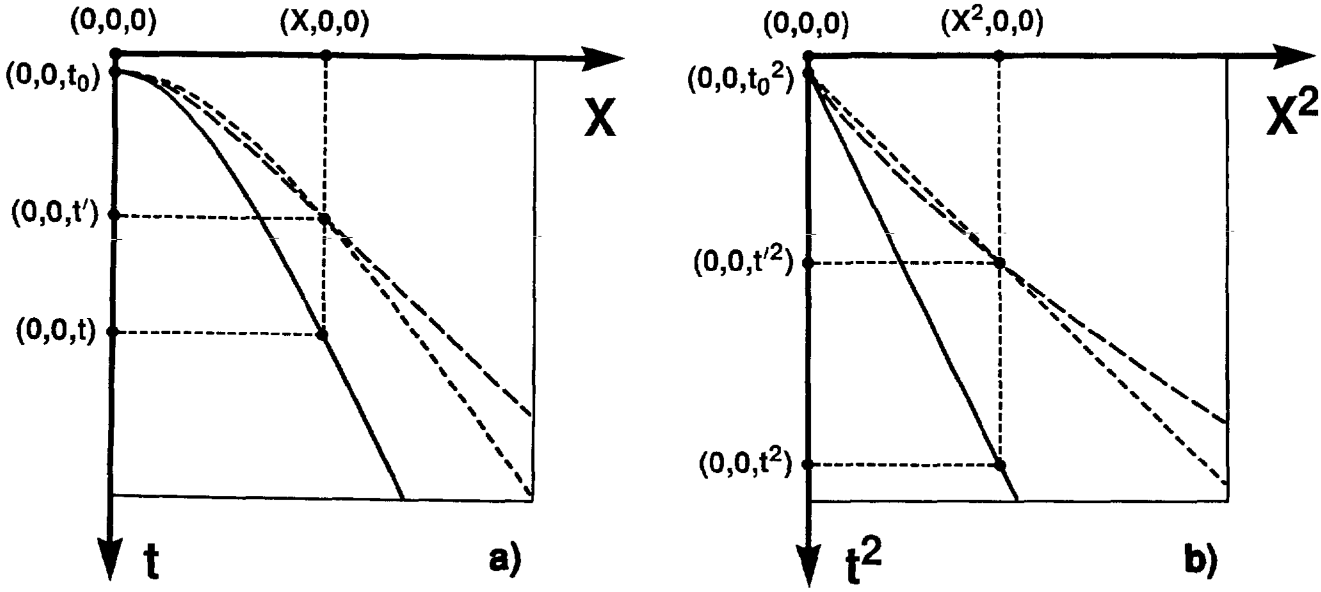

FIG. 2. Model transit time curves. (a) Solid curve relates transit time and midpoint position for both a uniform medium and straight rays in a stratified medium having an equivalent average velocity. Dashed curve describes true transit time-midpoint relation for a stratified medium. Dotted curve represents transit time-midpoint relation implied by equation (5). (b) Selected portion of corresponding curves in coordinates X^2 versus t^2.

$$V_{\text{rms}}^2 = \frac{1}{T_0} \sum_{k=1}^{n} v_k^2 \tau_k . \tag{9}$$

It can be demonstrated (Taner and Koehler, 1969) that equation (4), with $V = V_{\text{rms}}$, is a two-term truncation of the Taylor series expansion for $t^2(X)$ about the point $X = 0$. A third term, in X^4, is always negative, except in the limiting case where $v_1 = v_2 = , \ldots , = v_n$ or, equivalently, $V_{\text{rms}} = V_a = V$. This implies uniform velocity and all higher order terms beyond X^2 are zero.

In light of the foregoing discussion, let us now examine the nature of velocity estimates obtained from equations (5) and (6) for an in-plane scatterer where the v_k are not all equal. Although the actual event is known to be nonlinear in X^2 versus t^2, the estimate obtained by equation (5) assumes that it is linear. In other words, the resulting velocity estimate implies the hyperbola through (X, t') depicted in Figure 2a. Consequently, it is the slope of the corresponding line joining points $(0, t_0^2)$ and (X^2, t'^2) in Figure 2b that defines the velocity given by equation (5). Referring to the same figures, we can characterize the resulting estimate as follows. First, the velocity obtained is clearly dependent upon the variable X and increases as $|X|$. Second, it is obvious that this estimate will always exceed the average velocity defined by equation (7). Last, as we shall discover shortly, the estimate given by equation (5) can never exceed the generalized rms velocity, $V_{\text{rms}}(p_x)$, that is defined for the case $p_x = 0$ by equation (9). Although these observations provide a comparative context, we have yet to describe the meaning of the velocity furnished by equation (5). In fact, there is not much physical significance that can be attached to the estimate. The only description we can give is to say that it amounts to a very crude stacking velocity. If we assume that a stacking velocity V_s is defined by least squares fitting equation (4) to the observed event with $V = V_s$ (Al-Chalabi, 1973), we have

$$V_s^2 = \frac{4\left[m \sum_{i=1}^{m} X_i^4 - \left(\sum_{i=1}^{m} X_i^2 \right)^2 \right]}{m \sum_{i=1}^{m} t_i^2 X_i^2 - \sum_{i=1}^{m} t_i^2 \sum_{i=1}^{m} X_i^2}, \tag{10}$$

where m is the number of (X, t) pairs defining the estimate. Note that given just two points, $(0, t_0)$ and (X, t'), equation (10) reduces directly to equation (5). Unfortunately, as for the case of uniform velocity, there is little statistical significance associated with a two-point estimate.

Equation (6), on the other hand, yields a velocity estimate that is directly related to physical parameters. Returning to Figure 3, we observe that the midpoint variable X can be expressed in terms of discrete layer parameters as

$$X = \sum_{k=1}^{n} x_k = \frac{\cos \alpha}{2} \sum_{k=1}^{n} v_k t_k \sin \theta_k , \tag{11}$$

where $t_k = \tau_k / \cos \theta_k = \tau_k / (1 - p_x^2 v_k^2)^{1/2}$ is two-way transit time measured along the raypath within the kth layer, $x_k = (v_k t_k / 2) \sin \theta_k$ is the horizontal component of the raypath in the kth layer and θ_k is the angle between the ray and vertical. For the particular case of an in-plane scatterer, $\cos \alpha = 1$. Recalling that Snell's law requires the ray parameter $p_x = \sin \theta_k / v_k$ to be independent of layering, we can bring this constant outside the summation in equation (11) to yield

$$X = \frac{p_x \cos \alpha}{2} \sum_{k=1}^{n} v_k^2 t_k . \tag{12}$$

Finally, using equation (12) and recognizing that $t = \Sigma_{k=1}^{n} t_k$, we can rewrite equation (6) as

$$V^2 = \sum_{k=1}^{n} v_k^2 t_k \Bigg/ \sum_{k=1}^{n} t_k = V_{\text{rms}}^2(p_x). \tag{13}$$

We discover, as a result, that the velocity yielded by equation (6) is the same generalized rms velocity presented by Shah and Levin (1973). Moreover, as alluded to above, equation (13) reduces to Dix's rms velocity defined by equation (9) for the case $p_x = 0$. In addition to proving that $V_{\text{rms}}^2(p_x)$never decreases as X increases, Shah and Levin demonstrated that the generalized rms velocity is bounded, as expected, by the smallest and largest v_k in the section. The first of these conclusions follows from equation (6) and is tantamount to observing that the local slope of the event in X^2 versus t^2 is always decreasing (Figure 2a).

Following the lead of González-Serrano and Claerbout (1984) and Claerbout (1985), we realize that by incorporating the ray parameter, equation (6) also leads naturally to

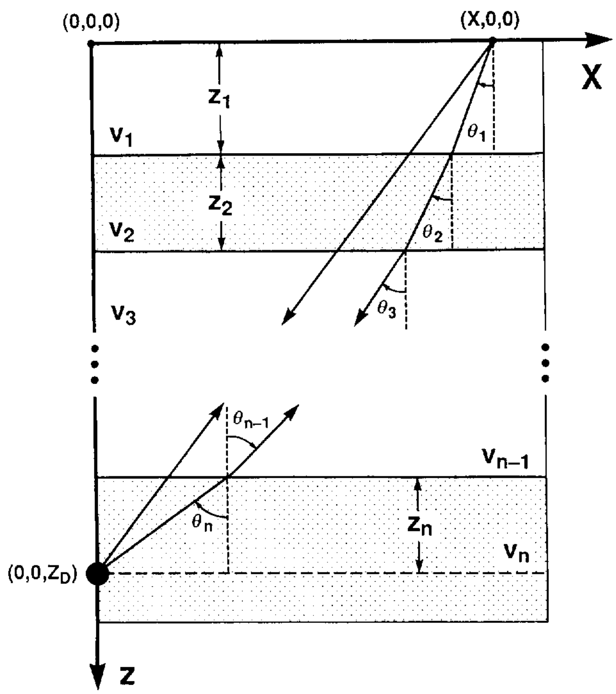

FIG. 3. Stratified earth model depicting both true and straight two-way raypaths joining a coincident source-receiver at $(X, 0, 0)$ with an in-plane diffractor at $(0, 0, Z_D)$. The v_k, z_k and θ_k $(k = 1, 2, 3, \ldots, n)$ denote velocity, thickness, and ray angle, respectively, for the kth layer.

interval velocities from two or more in-plane diffractions. In practice, we choose a tangent line having slope $dt/dX = 2p$ and subsequently determine, for each event, the respective point of tangency $(X, t(X))$, where X is measured relative to the respective apex. Now, treating the vertical interval between two in-plane scatterers as an effective unit having interval velocity v_i, it follows from equation (12) that

$$X_i - X_{i-1} = \frac{p}{2}\left[\sum_{k=1}^{i} v_k^2 t_k - \sum_{k=1}^{i-1} v_k^2 t_k\right] = \frac{p v_i^2 t_i}{2}. \tag{14}$$

Consequently, recognizing that the two-way transit time through the interval t_i must account exactly for the difference in total transit time,

$$t(X_i) - t(X_{i-1}) = \sum_{k=1}^{i} t_k - \sum_{k=1}^{i-1} t_k = t_i, \tag{15}$$

we find that the interval velocity can be obtained directly as

$$v_i^2(p) = \frac{2}{p}\frac{(X_i - X_{i-1})}{[t(X_i) - t(X_{i-1})]}. \tag{16}$$

Alternatively, upon establishing the tangent point for each event, we could have proceeded by evaluating equation (6) for the associated rms velocities. Then, with these in hand, the interval velocity follows from a straightforward re-expression of the previous equation

$$v_i^2(p) = \frac{V_{\mathrm{rms},i}^2(p)t(X_i) - V_{\mathrm{rms},i-1}^2(p)t(X_{i-1})}{t(X_i) - t(X_{i-1})}. \tag{17}$$

This expression reveals that v_i is, in particular, the rms interval velocity. Equation (17) is simply a generalization of the interval velocity due to Dix (1955) in the same sense that equations (13) and (9) are related (Nowroozi, 1989). The significance of rms interval velocities, compared with other varieties, has been discussed by Al-Chalabi (1974) and Hubral and Krey (1980). In short, although we view the interval as practically homogeneous, it generally includes some degree of velocity heterogeneity. We anticipate that intervals bounded by diffraction events are more likely to possess significant heterogeneity than those established on the basis of major reflection events. In fact, since reflection events are direct manifestations of velocity contrasts, we suggest that accompanying reflection information should aid in assessing the extent of velocity heterogeneity within an interval defined by diffractions. If heterogeneity is insignificant within the interval, its thickness is given by

$$z_i^2 = \frac{v_i(p)^2[t(X_i) - t(X_{i-1})]^2}{4} - (X_i - X_{i-1})^2. \tag{18}$$

LIMITATION FOR OUT OF PLANE DIFFRACTIONS

To this point, our treatment of a horizontally layered section has focused on scatterers residing in the plane of survey. We now emphasize that apart from our discussion of interval velocities, the foregoing analysis holds quite generally for an arbitrary scatterer. The velocity yielded by equation (6) is an estimate of the rms velocity described by equation (13) independent of the scatterer's location. Unfortunately, the estimate is of little use in the absence of associated depth control. As regards interval velocities, recall that the diffraction pattern for an arbitrary scatterer has local slope $dt/dX = 2p_x \cos\alpha$. Unlike the special case for in-plane diffraction events where $\cos\alpha = 1$, energy radiated from arbitrary scatterers via the same ray parameter cannot, in general, be identified on the basis of a unique local slope. Strictly speaking, even though the factor $\cos\alpha$ has less influence as p_x increases, the graphical method described above is appropriate only for in plane diffractions. Thus, to associate diffraction-based velocity estimates with a corresponding depth or stratigraphic unit, we must either assume that scatterers reside in plane or determine their true locations. For this reason, an obvious means of deriving the location of a scatterer from its expression on two or more profiles is described below. Although the result is only approximate for stratified media, we shall discover that the error is related to velocity heterogeneity. First, we return to the case of uniform velocity.

Consider, once again, a point diffractor within a constant velocity medium as depicted in Figure 1. Recall that our reference coordinate system was chosen such that the scatterer resides in the yz-plane. We found, on assuming coincident source-receiver, that the observed diffraction pattern is described exactly by equation (4). Consequently, the velocity predicted by equations (5) and (6), is independent of the scatterer's location. Having emphasized this, let us examine the significance of the constant t_0 in equation (4).

For a given event, $t_0 = 2r/V$ is the minimum arrival time for scattered energy detected by a coincident source-receiver. Recall that for a point scatterer at $(0, Y_D, Z_D)$, $r = (Y_D^2 + Z_D^2)^{1/2}$ is the length of a line segment joining the scatterer and the origin. It is important to appreciate that the diffraction event observed for this scatterer is not unique. The very same diffraction pattern would result for any scattering source located at $(0, y, z)$ satisfying $y^2 + z^2 = r^2 = Y_D^2 + Z_D^2$; that is, for any scatterer residing on a semicircle of radius r from the origin in the yz-plane. It follows that upon identifying events having a common source on two or more optimum offset profiles, the scattering source may be located identically. Profiles need not be parallel but this aids in identifying common events since their apexes must occur at the same traverse position. The strategy is illustrated in Figure 4 for a profile acquired along the x-axis ($y = 0$) and a second parallel profile at $y = Y$. Assuming common diffraction events have been identified on both records and velocity estimates subsequently obtained, arcs of radii $r_{y=0} = Vt_{0,0}/2$ and $r_{y=Y} = Vt_{0,Y}/2$ are constructed from respective centers, $y = 0$ and $y = Y$. The scatterer is located at the intersection of the resulting arcs.

Prior to examining the analogous scenario for a true stratified media, it is again useful to consider the hypothetical case of straight rays in a uniform medium having the effective average velocity. Under this assumption, equation (4) continues to describe the resulting diffraction pattern if we only replace the constant velocity V by the average velocity defined by equation (7). Using average velocity estimates from events observed for $y = 0$ and $y = Y$, we could proceed as described above. Intersection of the resulting arcs would once again imply the scatterer's location as illustrated in Figure 5. We have also depicted what we shall call "straight ray wavefronts" for $t_{0,0}$ and $t_{0,Y}$. These are just the loci of endpoints for straight rays that leave a given source at arbitrary take-off angles and are extended at the appropriate layer velocities for half the corresponding apex time. We observe that the intersection of these so-called wavefronts and, consequently, the scatterer's true location coincides with that of the experimentally determined arcs. In other words, if the straight ray assumption were valid, our simple strategy would also properly locate scatterers within stratified media.

We turn now to the actual situation for a horizontally layered section. Recall that the observed diffraction event is really a record of transit time for scattered energy that takes the path of least time to and from the scatterer as a function of X. Here, equation (4) approximately describes the actual event on replacing the constant velocity V by Dix's rms velocity or what amounts to equation (13) evaluated for $p_x = 0$. In practice, however, equation (6) yields the generalized rms velocity for some nonzero Snell parameters. Consequently, for the purpose of determining the scatterer's location in the yz-plane, this estimate should be obtained for X as small as possible since $V_{\text{rms}}(p_x)$ increases with X.

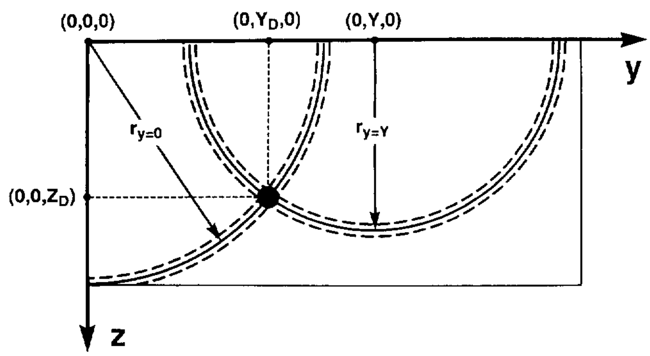

FIG. 4. Location of point scatterer in uniform medium from two optimum offset profiles parallel to the x-axis at $y = 0$ and $y = Y$. Scatterer's position $(0,\ Y_D, Z_D)$ is indicated by intersection of circular wavefronts having radii $r_{y=0}$ and $r_{y=Y}$. Dashed curves are a qualitative suggestion of uncertainty.

Practically speaking, however, caution is advised since local slope estimates are obviously subject to greater error as X decreases. Having issued this warning, let us suppose for the time being that we are able to estimate the appropriate rms velocities at $X = 0$ for the pair of diffraction events considered in the foregoing examples. Arcs having the appropriate radii are subsequently constructed as illustrated in Figure 6. We have also displayed the true wavefronts for $t_{0,0}$ and $t_{0,Y}$. Like the hypothetical straight ray wavefronts in Figure 5, intersection of these wavefronts marks the actual location of the scatterer. But, in contrast to the previous examples, intersection of the experimentally derived arcs only approximately locates the scatterer. To provide a sense of scale, the model parameters resulting in Figures 5 and 6 are as follows: $Y_D = 60.0$ m, $Z_D = 50.0$ m, $z_1 = 10.0$ m, $v_1 = 750.0$ m/s, $z_2 = 20.0$ m, $v_2 = 1500.0$ m/s, $z_3 = Z_D - (z_1 + z_2) = 20.0$ m, $v_3 = 2500.0$ m/s. The predicted location is $Y_D = 65.1$ m, $Z_D = 62.1$ m.

The error is related to the difference between rms and average velocities. A measure of this difference can be expressed as

$$g(p_x) = \frac{V_{\text{rms}}^2(p_x) - V_a^2}{V_a^2} = \frac{\displaystyle\sum_{k=1}^{n} \frac{z_k}{v_k} \sum_{j=1}^{n} \frac{z_j}{v_j} \sum_{i=1}^{n} \frac{z_i}{v_i} \frac{(v_i^2 - v_k v_j)}{(1 - p_x^2 v_i^2)^{1/2}}}{\displaystyle Z_D^2 \sum_{i=1}^{n} \frac{z_i}{v_i} (1 - p_x^2 v_i^2)^{-1/2}}, \tag{19}$$

where the Snell parameter p_x is, in general, different for profiles at $y = 0$ and $y = Y$. Recalling that rms velocity always exceeds the corresponding average velocity, we recognize that this quantity must be strictly positive. In other words, neglecting other sources of error, the predicted depth for a given scatterer will always exceed the true value. Moreover, the sign of the corresponding error in Y_D depends on the relative magnitude of $r_{y=0}$ and $r_{y=Y}$. In particular, for $r_{y=0} = r_{y=Y}$, the error is zero. Although, in practice, a quantitative assessment of these errors will be difficult at

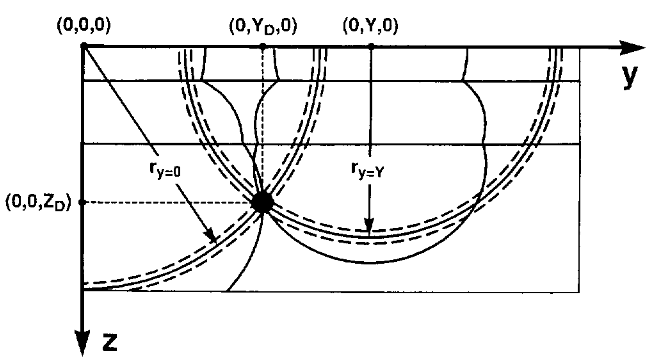

FIG. 5. Location of point scatterer in stratified medium assuming straight rays. Intersection of circular wavefronts based on average velocity estimates coincides with that of "straight ray wavefronts" at the scatterer's location.

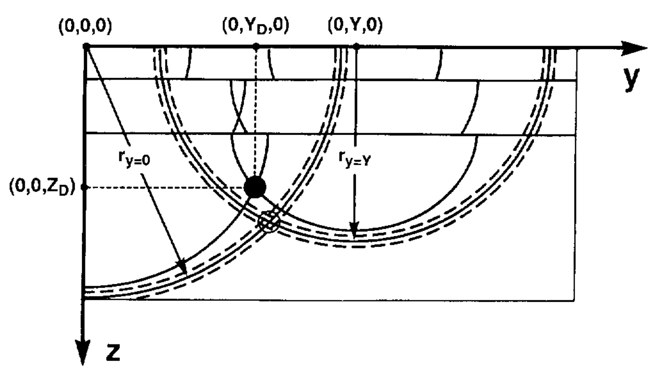

FIG. 6. Approximate location of scatterer in stratified medium respecting Snell's law. Intersection of circular wavefronts based on rms velocity estimates fails to coincide with that of true wavefronts at the scatterer's location.

best, there is an important qualitative relationship between the accuracy that can be expected and the velocity structure of the subsurface. For $p_x = 0$, equation (19) can be re-expressed as

$$g(0) = \frac{V_{\rm rms}^2(0) - V_a^2}{V_a^2} = \frac{1}{Z_D^2} \sum_{k=1}^{n-1} z_k \sum_{j=k+1}^{n} z_j \frac{(v_k - v_j)^2}{v_k v_j}. \tag{20}$$

Al-Chalabi (1974) used the term heterogeneity factor to describe this quantity, $g(0)$, since it characterizes the velocity heterogeneity of the subsurface. Where stratification is characterized by sparse but large velocity contrasts, the heterogeneity factor and more generally equation (19) will have large values. Consequently, we find that the uncertainty in our method for locating a scatterer is directly related to velocity heterogeneity. In particular, for the model parameters cited above, the heterogeneity factor has a value of $g(0) = 0.2133$. For comparison, the same model with weaker velocity stratification ($v_1 = 750.0$ m/s, $v_2 = 1000.0$ m/s, $v_3 = 1250.0$ m/s) has a heterogeneity factor of $g(0) = 0.0360$. In this case, the location procedure yields $Y_D = 61.3$ m, $Z_D = 52.7$ m. The improvement suggests that in many situations, particularly where diffractions have their origin within unconsolidated overburden, the procedure described here can yield an accurate location and consequently reliable depth control for the associated velocity estimate.

Before proceeding, we return briefly to the assumption that velocity estimates could be obtained, using equation (6) at $X = 0$. As cautioned above, this cannot be achieved in practice and, consequently, the scatterer's predicted location is subject to additional error. One means of reducing this added error is to obtain two or more velocity estimates for a given event at acceptable values of X and perform an appropriate extrapolation for the corresponding $V_{\rm rms}(p_x = 0)$. We shall return to this issue in following sections.

EFFECT OF NONZERO OFFSET

The foregoing discussion and analysis of velocities from diffractions has assumed that source and receiver are coincident. Although one might expect that this assumption is warranted in interpreting ground penetrating radar data, that it is also appropriate for shallow seismic data is less evident. Let us now examine the effect of nonzero optimum offset on measured transit time as a function of midpoint position and the resulting influence on velocity estimates yielded by equation (6). Referring again to Figure 1, consider a point scatterer within a uniform velocity medium at a distance $r = (Y_D^2 + Z_D^2)^{1/2}$ from the origin. Recall that equation (3) describes the two-way transit time at midpoint location $X_M = (X_R + X_S)/2$ as measured by a source-receiver pair located at $(X_S, 0, 0)$ and $(X_R, 0, 0)$, respectively, and separated by an optimum offset $\Delta x = X_R - X_S$. As this offset approaches zero, the transit time approaches that given by equation (4) and it is from this relation that equations (5) and (6) derive.

In Figure 7a, we present a set of characteristic curves that specify the difference between zero offset and nonzero offset transit times Δt as a function of X_M/r for $\Delta x/r$ ranging from 0.1 to 50.0. Notice that the transit time difference is normalized by the normal incidence transit time $t_0 = 2r/V$ and that the vertical axis is displayed in logarithmic format. These curves are symmetric about $X_M/r = 0$ and quantify the so-called Cheop's pyramid effect described by Claerbout (1985). The effect is especially evident for large values of $\Delta x/r$ where relatively stable plateaus near $X_M/r = 0$ reflect the severely truncated apexes of the corresponding diffraction event for $|X_M/\Delta x| \le 0.5$. In absolute terms, we observe that the deviation between zero offset and nonzero offset transit times at $X_M/r = 0$ ranges from approximately 0.1 percent of normal incidence time for $\Delta x/r = 0.1$ to nearly fifty times normal incidence time for $\Delta x/r = 50.0$. For $\Delta x/r \le 5.0$, however, this error decreases rapidly as X_M/r increases. Of course, these departures from the hyperbolic nature of scattering events also influence velocity estimates predicted by equation (6) since this expression involves the local slope of the diffraction pattern. This influence is characterized by the corresponding curves displayed in Figure 7b. Here the deviation of the predicted velocity from the true value, ΔV, is charted as a function of X_M/r for the same range of $\Delta x/r$. In this case, the deviation is normalized by the true velocity. Not surprisingly, the gross character of these curves resembles those for the corresponding transit time disparities but, in general, the relative error in predicted velocities is somewhat less and decreases more rapidly as $\Delta x/r$ increases. From a practical perspective, these characteristic curves indicate that the error introduced by nonzero optimum offset is not prohibitively large except where $\Delta x/r$ is very large. Otherwise, so long as we apply equation (6) at a reasonable distance from the apex of a diffraction event, the resulting error is quite acceptable. As a rule of thumb, estimates should not be made for $|X/\Delta x| < 0.5$ and preferably for $|X/\Delta x| \ge 2.0$. Respecting this constraint, the error in predicted velocities resulting from nonzero optimum offset never exceeds 1.0 percent. An intermediate condition $|X_M/\Delta x| \ge 1.0$ also limits error to 1.0 percent except over the range $0.25 \le \Delta x/r \le 5.0$ where maximum error approaches 5.0 percent. Unfortunately, this is precisely the range most frequently encountered in shallow seismology. Curves illustrating these criteria are displayed in Figure 7b.

Finally, computational analysis indicates that inflation of velocity estimates resulting for nonzero optimum offset increases with velocity heterogeneity. In other words, Figure 7b should be viewed as characterizing the limiting condition for $g(0) = 0.0$. Let us return, for example, to the situation considered in connection with Figures 4, 5, and 6. If we assume that $v_1 = v_2 = v_3$ and an optimum offset of 50.0 m, Figure 7b predicts that the velocity estimate yielded by equation (6) incorporates a maximum error of $\Delta V/V \approx 0.05$ due to offset. In comparison, the velocity model used to generate Figures 5 and 6 ($v_1 = 750.0$ m/s, $v_2 = 1500.0$ m/s, $v_3 = 2500.0$ m/s) has a heterogeneity factor of $g(0) = 0.2133$ and yields a computed error of $\Delta V_{\rm rms}/V_{\rm rms}(p_x = 0) \approx 0.085$. In turn, the more weakly stratified model ($v_1 = 750.0$ m/s, $v_2 = 1000.0$ m/s, $v_3 = 1250.0$ m/s), having a heterogeneity factor of $g(0) = 0.0360$, results in an intermediate error of $\Delta V_{\rm rms}/V_{\rm rms}(p_x = 0) \approx 0.065$. We qualify these findings by stating that for all cases examined, the influence of velocity heterogeneity diminishes rapidly as X_M/r increases. In particular, for the cases cited above, the departure of observed error from that predicted by Figure 7b becomes practically negligible by $X_M/r = 2.0$. Bearing this in mind, we re-emphasize that the effect of nonzero offset is not the only consideration restricting velocity estimates near $X = 0$. As alluded to earlier, elevated uncertainty in the measurement of local event slope dt/dX in the region about $X = 0$ imposes an additional limitation.

CONCLUDING DISCUSSION

In closing, we present a purely demonstrative example to illustrate the mechanics of the method. Figure 8 is a portion of an optimum offset section (BB-900) acquired by the Geological Survey of Canada on the Fraser River delta, British Columbia (Pullan et al., 1989). The format is the same as for Figure 2a with the origin located directly over the apex of the analyzed scattering event at approximately 67.5 ms. The optimum offset was 24.0 m and the trace interval is 3.0 m.

Local tangents to the diffraction pattern are established at distances of $X_1 = 45.0$ m, $X_2 = 60.0$ m and $X_3 = 75.0$ m from the origin. These tangents have measured slopes of $(dt/dx)_1 = 0.595$ ms/m, $(dt/dx)_2 = 0.673$ ms/m and $(dt/dx)_3 = 0.733$ ms/m. The respective two-way transit times are $t_1 = 81.9$ ms, $t_2 = 91.1$ ms, and $t_3 = 100.8$ ms. Using these values, equation (6) yields corresponding rms velocities of approximately $V_1 = 1922$ m/s, $V_2 = 1979$ m/s, and $V_3 = 2015$ m/s. That these estimates increase with distance from the origin is consistent with our analysis of stratified media and, consequently, we view these estimates as generalized rms velocities defined by equation (13). Moreover, as we have only marginally violated the restriction $|X/\Delta x| \geq 2$ and there is no seismic evidence for strong velocity heterogeneity, these estimates should be accurate to within about 1 percent of the true rms velocities. Of course, the presence of uncertainties in the measured values cited above produces additional error. In the present case, we estimate that this additional error is less than 5 percent but may approach 10 percent, depending on the quality of data. An accompanying depth scale supplied by Pullan et al. and based on a series of borehole velocity surveys, places the apex of the diffraction event at about 53.0 m and implies an average velocity of approximately 1570 m/s to this depth. To furnish a comparison with our findings, we perform a simple extrapolation to project the rms velocity at $X = 0$ from our estimates at $X = 45.0$, 60.0 and 75.0 meters. Neglecting measurement errors, least-squares linear extrapolation yields an estimate of 1786 m/s. Assuming an in-plane scatterer ($p_x = 0$ for $X = 0$), the difference between this estimate and the average velocity determined by Pullan et al. implies a heterogeneity factor of approximately $g(0) = 0.29$. However, since there is no apparent evidence for significant velocity heterogeneity, this value suggests that either the average velocity or the rms velocity is in error.

Numerous sources of error exist. For example, the average velocity structure used by Pullan et al. to generate the accompanying depth scale ignores the existence of lateral

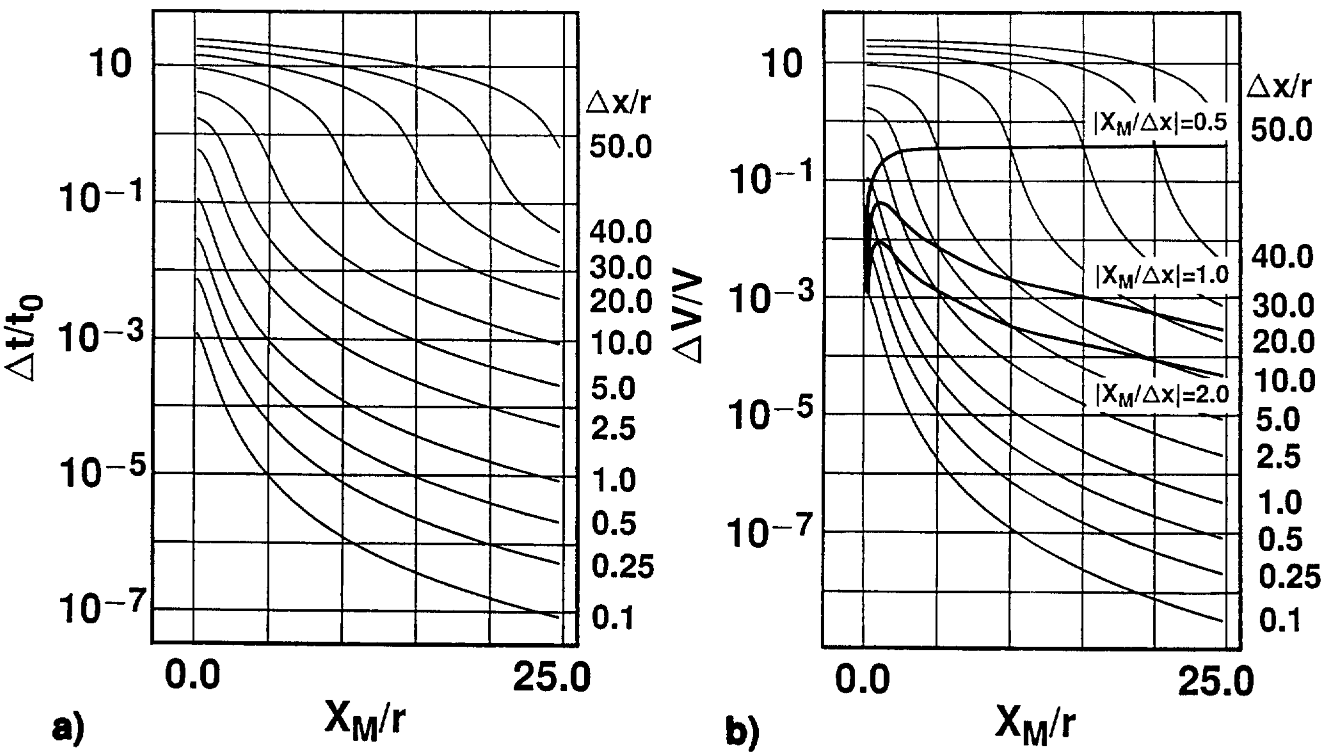

FIG. 7. Effect of nonzero optimum offset for uniform media. (a) Normalized transit time error $\Delta t = (t(\Delta x \neq 0) - t(\Delta x = 0))/t_0(\Delta x = 0)$. (b) Corresponding normalized velocity error $\Delta V = (V_{\text{est.}} - V_{\text{true}})/V_{\text{true}}$ (bold curves display criteria related to expected error limits). Transit time and velocity errors are displayed versus midpoint position scaled by distance from origin to scatterer. Curves are depicted for various ratios of offset to distance.

velocity variations and this suggests the utility of diffraction-based estimates for local velocity control. Inconsistent velocities can also arise from diffractions occurring out of plane but, ordinarily, these events imply a velocity and, thus, a heterogeneity factor that is too low rather than high. In addition, modeling indicates that linear extrapolations yield results that are almost invariably too high. We have found that the consistency between predicted rms and average velocities can be improved in many cases by a more sophisticated extrapolation. These approaches can also backfire, however, primarily due to the effect of nonzero optimum offset. Finally, it is conceivable that the observed discrepancy arises purely from uncertainties in transit time and local slope measurements.

In addition to illustrating the method we have described for diffraction-based velocity estimation, the foregoing example also suggests limitations on the interpretation of velocity estimates derived from a single diffraction. More substantial conclusions and improved confidence can be obtained by analyzing additional scattering events or multiple profiles.

ACKNOWLEDGMENTS

The authors are grateful to S. E. Pullan and J. A. Hunter for permission to use data from the 1987 Fraser delta survey and to D. F. Aldridge for useful comments on a first draft of this manuscript.

REFERENCES

Al-Chalabi, M., 1973, Series approximation in velocity and traveltime computations: Geophys. Prosp., **21**, 783–795.
Al-Chalabi, M., 1974, An analysis of stacking, rms, average, and interval velocities over a horizontally layered ground: Geophys. Prosp., **22**, 458–475.
Claerbout, J. F., 1985, Imaging the Earth's interior: Blackwell Scientific Publications, Inc.
Daniels, J. J., 1989, Fundamentals of ground penetrating radar: Proc., Symp. on Application of Geophysics to Engineering and Environmental Problems, Soc. Engr. and Min. Expl. Geophys., 62–142.
Dinstel, W. L., 1971, Velocity spectra and diffraction patterns: Geophysics, **36**, 415–417.
Dix, C. H., 1955, Seismic velocities from surface measurements: Geophysics, **20**, 68–86.
González-Serrano, A., and Claerbout, J. F., 1984, Wave-equation velocity analysis: Geophysics, **49**, 1432–1456.

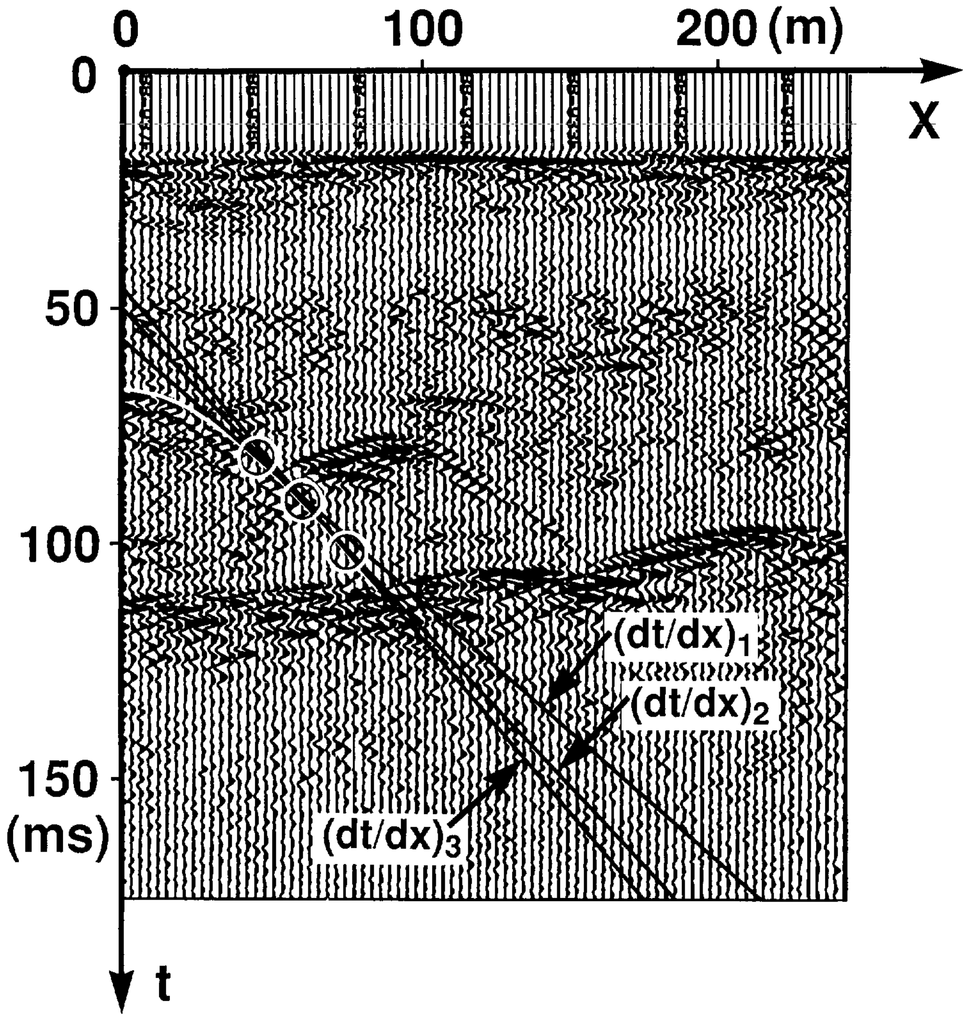

FIG. 8. Portion of optimum offset profile acquired on the Fraser River delta, British Columbia. Tangents to the diffraction pattern at circled points have slopes $(dt/dx)_1$, $(dt/dx)_2$, and $(dt/dx)_3$.

Hubral, P., and Krey, T., 1980, Interval velocities from seismic reflection time measurements: Soc. Expl. Geophys.

Hunter, J. A., Pullan, S. E., Burns, R. A., Gagne, R. M., and Good, R. L., 1984, Shallow seismic reflection mapping of the overburden-bedrock interface with the engineering seismograph—some simple techniques: Geophysics, **49**, 1381–1385.

Hunter, J. A., and Pullan, S. E., 1989, The optimum offset shallow seismic reflection technique: Proc., Symp. on Application of Geophysics to Engineering and Environmental Problems, Soc. Engr. and Min. Expl. Geophys., 143–174.

Knapp, R. W., and Steeples, D. W., 1986, High-resolution common depth point seismic reflection profiling: field acquisition parameter design: Geophysics, **51**, 283–294.

Larner, K., Chambers, R., Yang, M., Lynn, W., and Wai, W., 1983, Coherent noise in marine seismic data: Geophysics, **48**, 854–886.

Levin, F. K., 1971, Apparent velocity from dipping interface reflections: Geophysics, **36**, 510–516.

Nowroozi, A. A., 1989, *Generalized form of the Dix equation for the* calculation of interval velocities and layer thicknesses: Geophysics, **54**, 659–661.

Pullan, S. E., Jol, R. M., Gagne, R. M., and Hunter, J. A., 1989, Compilation of high resolution optimum offset shallow seismic reflection profiles from the southern Fraser River delta, British Columbia: Geol. Surv. Can., open file #1992.

Shah, P. M., and Levin, F. K., 1973, Gross properties of time-distance curves: Geophysics, **38**, 643–656.

Steeples, D. W., and Miller, R. D., 1988, Seismic reflection methods applied to engineering, environmental, and ground-water problems: Proc., Symp. on Application of Geophysics to Engineering and Environmental Problems, Soc. Engr. and Min. Expl. Geophys., 1–52.

Taner, M. T., and Koehler, F., 1969, Velocity spectra-digital computer derivation and applications of velocity functions: Geophysics, **34**, 859–881.

Tsai, C. J., 1984, An analysis leading to the reduction of scattered noise on deep marine seismic records: Geophysics, **49**, 17–26.

Ulriksen, C. P. F., 1982, Application of impulse radar to civil engineering: Ph. D. Thesis, Lund Univ. of Tech., Published in U. S. A. by Geophysical Survey Systems, Inc.